Received: 14 January 2020 | Revised: 22 April 2020 | Accepted: 24 April 2020

DOI: 10.1002/stem.3204

REGENERATIVE MEDICINE

STEM CELLS

Exosomal miRNA-17-5p derived from human umbilical cord mesenchymal stem cells improves ovarian function in premature ovarian insufficiency by regulating SIRT7

Chenyue Ding[1] | Liping Zhu[3] | Han Shen[2] | Jiafeng Lu[1] | Qinyan Zou[1] | Chao Huang[1] | Hong Li[1] | Boxian Huang[1,2]

[1]Center of Reproduction and Genetics, Affiliated Suzhou Hospital of Nanjing Medical University, Suzhou Municipal Hospital, Suzhou, People's Republic of China

[2]State Key Laboratory of Reproductive Medicine, Nanjing Medical University, Nanjing, People's Republic of China

[3]Department of Obstetrics and Gynecology, Suzhou Hospital Affiliated to Nanjing Medical University, Suzhou, People's Republic of China

Correspondences

Email: huangboxiannj@163.com (Boxian Huang);

Email: hongliszivf@163.com (Hong Li); **Boxian Huang** Address: Center of Reproduction and Genetics, Affiliated Suzhou Hospital of Nanjing Medical University, Suzhou Municipal Hospital, Suzhou, 215002, China,

Tel: +86-512-62362461,

Fax: +86-512-62362461,

E-mail: huangboxiannj@163.com; **Hong Li** Address: Center of Reproduction and Genetics, Affiliated Suzhou Hospital of Nanjing Medical University, Suzhou Municipal Hospital, Suzhou, 215002, People's Republic of China.

Tel: +86-512-62362461,

Fax: +86-512-62362461,

E-mail: hongliszivf@163.com

Abstract

Premature ovarian insufficiency (POI) is clinically irreversible in women over 40. Although numerous studies have demonstrated satisfactory outcomes of mesenchymal stem cell therapy, the underlying therapeutic mechanism remains unclear. Exosomes were collected from the culture medium of human umbilical cord mesenchymal stem cells (hUMSCs) and assessed by electron microscopy and western blot (WB) analysis. Then, exosomes were added to the culture medium of cyclophosphamide (CTX)-damaged human granulosa cells (hGCs), and the mixture was injected into the ovaries of CTX-induced POI model mice before detection of antiapoptotic and apoptotic gene expression. Next, the microRNA expression profiles of hUMSC-derived exosomes (hUMSC-Exos) were detected by small RNA sequencing. The ameliorative effect of exosomal microRNA-17-5P (miR-17-5P) was demonstrated by miR-17-5P knockdown before assessment of ovarian phenotype and function, reactive oxygen species (ROS) levels and SIRT7 expression. Finally, SIRT7 was inhibited or overexpressed by RNA interference or retrovirus transduction, and the protein expression of PARP1, γH2AX, and XRCC6 was analyzed. The ameliorative effect of hUMSC-Exos on POI was validated. Our results illustrated that hUMSC-Exos restored ovarian phenotype and function in a POI mouse model, promoted proliferation of CTX-damaged hGCs and ovarian cells, and alleviated ROS accumulation by delivering exosomal miR-17-5P and inhibiting SIRT7 expression. Moreover, our findings elucidated that miR-17-5P repressed PARP1, γH2AX, and XRCC6 by inhibiting SIRT7. Our findings suggest a critical role for exosomal miR-17-5P and its downstream target mRNA SIRT7 in hUMSC transplantation therapy. This study indicates the promise of exosome-based therapy for POI treatment.

KEYWORDS

Exosomes, Human umbilical cord mesenchymal stem cells, miR-17-5p, Premature ovarian insufficiency, SIRT7

[†] These authors contributed equally to this work

1 | INTRODUCTION

Premature ovarian insufficiency (POI), also known as premature ovarian failure (POF), is characterized by oocyte apoptosis, follicular atresia, menstruation cessation and elevated plasma levels of follicle-stimulating hormone (FSH), and the condition affects 1% of women worldwide by the age of 40 (1). Although women with POF may become pregnant after hormone replacement therapy and ovulation induction (2), POF is clinically irreversible. In addition, hormone replacement therapy increases the risk of cancer and posttreatment recurrence, forcing patients to look for alternative therapies (3).

The multiple etiologies of POI include genetic factors, autoimmunity, infection and idiopathic factors (4). Mitochondrial abnormalities and oxidative stress (OS) have also been demonstrated to be related to follicular atresia and POI (5-7). The past decade has witnessed satisfactory outcomes of treatment with various types of mesenchymal stem cells (MSCs) with regard to rescue of ovarian function in POI models (8-11). Among MSCs, human umbilical cord MSCs (hUMSCs) have been widely studied because of their easy isolation methods, low immunogenicity, high proliferative capacity and self-renewal ability. However, the mechanisms by which transplanted hUMSCs restore ovarian function, improve follicular development and regulate immunity remain unclear (12,13).

One of the key mechanisms of MSC-induced therapeutic effects is the paracrine activity of secreted factors, which are mediated by extracellular vesicles (EVs) (10,14,15). Among the many subtypes of EVs, exosomes are considered to be powerful cell-to-cell communication-relevant components of the MSC secretome with low immunogenicity and tumorigenicity (16,17). Exosomes released from hUMSCs (hUMSC-Exos) are reported to suppress ovarian granulosa cell apoptosis and regulate the immune response (18,19). These small 40-150 nm EVs carrying microRNAs (miRNAs) that regulate gene expression may replace cell-based therapies for POI treatment.

An exosomal miRNA (miR-10a) from amniotic fluid stem cells has been reported to rescue cyclophosphamide (CTX)-induced POF (20). In addition, the hUMSC-derived exosomal miRNAs miR-100 and miR-146a can accelerate vaginal epithelial cell proliferation (21). Moreover, miRNAs including miR-93, miR-34a, miR-214, and miR-217 have been reported to control reactive oxygen species (ROS) levels in OS-driven aging diseases (22). Nevertheless, the miRNA expression profile of hUMSC-Exos and the downstream target mRNAs have never been investigated.

miRNA-17-5P (miR-17-5P) has been reported to be a key regulator of the G1/S phase cell cycle transition (23). Moreover, miR-17-5P overexpression suppresses apoptosis and promotes proliferation, migration and invasion of ovarian cancer cells (24). Sirtuins, which are divided into 7 classes (SIRT1 to SIRT7), are major regulators of cellular responses to metabolic, oxidative and genotoxic stresses (25). SIRT7 deficiency contributes to accelerated aging and defective embryogenesis (25,26). However, there is a lack of understanding about the mechanisms by which SIRT7 and miR-17-5P alleviate POI and regulate OS-related activities. In addition, the interaction between miR-17-5P and SIRT7 has never been investigated.

Significance Statement

our findings reveal that hUMSC-Exos rescue POI and repress ROS accumulation by downregulating the expression of SIRT7 and its downstream target genes (PARP1,? H2AX and XRCC6) via delivery of exosomal miR-17-5P. This study not only clarifies the underlying mechanism of hUMSC-Exos treatment but also provides insight into the potential of exosomal miRNA-based therapy.

In this study, hUMSC-Exos inhibited apoptosis of CTX-damaged human granulosa cells (hGCs), alleviated OS and rescued ovarian phenotype and function in a CTX-induced POI mouse model. Moreover, hUMSC-Exos suppressed the expression of SIRT7 and its downstream target gene by activating miR-17-5P.

2 | MATERIALS AND METHODS

2.1 | Isolation and Culture of hUMSCs

hUMSCs were obtained from Suzhou Municipal Hospital. Informed consent was given by donors before their full-term umbilical cords were obtained. Briefly, the digested cells were seeded in 10 cm^2 culture dishes at a density of 1×10^7 cells/cm^2 and cultured in an incubator at 37°C with 5% CO_2. The isolated cells were fed every third day. After removing nonadherent cells, hUMSCs were obtained. Cells at passages 3-5 were used for this study.

2.2 | Isolation of Primary hGCs from POI Patients

hGCs were voluntarily donated by POI patients. The ethics committee of Suzhou Municipal Hospital approved the use of hGCs for the following experiments. All patients were informed, and written consent was obtained. All information about the samples and patients was anonymized. After centrifugation at 560 × *g* for 3 min, hGCs were isolated. Then, the hGCs were washed in serum-free DMEM/F12 medium 3 times. Next, the hGCs were cultured in DMEM/F12 medium supplemented with 10% FBS. The following experiments were conducted on the third day after cell culture.

2.3 | Preparation of hUMSC-Exos

Exosomes were obtained from the culture medium of hUMSCs. In detail, hUMSCs at passage 3 were seeded on culture plates and reached 80% confluence at 5 days. Then, conditioned medium with exosome-depleted FBS (Thermo Fisher, USA) was collected after culturing for 48 h. To remove cells, the collected medium was

centrifuged at 300 × *g* for 10 min at 4°C followed by filtration through 0.22 μm filters. Then, the supernatant was centrifuged at 3000 × *g* for 15 min at 4°C to again filter cells and debris. The supernatant was collected carefully and mixed with ExoQuick precipitation solution (SBI, USA). After incubating the mixture overnight at 4°C, exosomes were isolated by centrifugation at 1500 × *g* for 30 min at 4°C. The formed exosome pellets were dissolved in PBS before being added to the culture medium of CTX-damaged hGCs. The exosomes were labeled with CM-DiI Dye (Sigma-Aldrich, USA), a molecular probe, following the manufacturer's instructions before injection into the POI model mice.

2.4 | Experimental Animals and POI Mouse Model Establishment

All the experimental procedures in this study were conducted following the recommendations of the Association for Research in Reproductive Function and were approved by the Ethics Committee of Nanjing Medical University (approval number: 20170480). Ten-week-old female specific pathogen-free (SPF)-grade C57B6L/J mice were purchased from the Institute of Animal Research at Nanjing Medical University. In this study, the mice were equally and randomly divided into four groups: the wild-type (WT) group (n = 10), the CTX-induced POI model group (POI group, n = 10), the CTX-induced POI model group treated with exosomes from hUMSCs (Exos/POI group, n = 10), and the CTX-induced POI model group treated with exosomes from miR-17-5P-knockdown hUMSCs (hUMSC-miR-17-5P^{KD}) (Exos$^{anti\text{-}miR\text{-}17\text{-}5p}$/POI group, n = 10). The WT mice were not given any treatment. To establish the POI mouse model, CTX (Sigma, USA) was injected at a dose of 120 mg/kg. At least three biological replicates were used during the experiments. The operators were blinded to the treatment during data acquisition and analysis.

2.5 | Gene Overexpression via Retrovirus Transduction

To overexpress SIRT7 in hGCs, we amplified the SIRT7 coding sequence from human gDNA. Then, we cloned the SIRT7 coding sequence into the BglII and SalI sites of the retroviral vector pLNCX2 (Clontech, USA) at a multiplicity of infection (MOI) of 5. Retrovirus transduction was performed by culturing hUMSCs with retroviral or control plasmids in a 37°C incubator with 5% CO_2 for 48 h. Then, the cells were centrifuged at 1000 × *g* for 10 min to remove residual retrovirus in the supernatant. Next, the hUMSCs were cultured with medium containing 1000 mg/mL G418 for 2 weeks to select retrovirus-infected cells. SIRT7 overexpression was measured by detecting target protein levels.

2.6 | Ovarian Follicle Counting

At 4 weeks post transplantation, the mice were euthanized, and the bilateral ovaries were removed and fixed in 10% paraformaldehyde for 2 h. Then, the ovaries were embedded in paraffin and sectioned with a thickness of 5 μm. Five sections were collected from each ovary. The ovarian structure and follicle phenotype were shown by staining with hematoxylin and eosin (HE). The total follicles and antral follicles were counted. Every follicle containing an oocyte was counted once to avoid recounting. Every experiment was repeated at least three times. The results are presented as the fold change ± SD. $P < 0.05$ was considered to indicate significance.

2.7 | Metabolite Assay

For the metabolite assay, 0, 24, 48, and 72 h-cultured hGCs were extracted. The levels of triglyceride (Triglyceride Assay Kit, Abcam, USA), glycogen (Glycogen Assay Kit II, Abcam, USA), trehalose (Trehalose Assay Kit, MyBioSource, USA) and glucose (Glucose Assay Kit, Abcam, USA) were quantified by a spectrophotometer (Varian Company, Australia) following the instructions. A minimum of three assays were performed, and the outcomes are shown as the fold change ± SD. $P < 0.05$ indicated significance.

3 | RESULT

3.1 | hUMSC-Derived Exosomes Rescued CTX-Damaged hGCs and Ovaries from Apoptosis

First, exosomes were obtained from hUMSCs using conventional differentiation centrifugation methods. hUMSC-Exos were confirmed as mean diameters of 141.6 nm and revealed the classic characterization of cup-shaped morphology (Figure S1A-B). The protein-level expression of classical exosomal markers (CD9, CD63, and CD81) was detected in isolated hUMSC-Exos (Figure S1C). Besides, FACS method indicated that the hUMSCs and hUMSC-Exos group were expressed the markers CD9, CD63 and CD81 as shown in Figure S1D.

To verify the restorative role of hUMSC-Exos and the optimal treatment dose, four doses of hUMSC-Exos (0 particles/ml, 10^{10} particles/ml, 5×10^{10} particles/ml and 10^{11} particles/ml) were added to the culture medium of CTX-damaged hGCs for 48 h. We detected the expression of proliferation markers (PCNA and KI67) using FACS, and our results demonstrated that the proliferation rates of CTX-damaged hGCs were dramatically upregulated in the 5×10^{10} (57.7%) and 10^{11} particles/ml groups (78.1%) compared with the 0 particles/ml group (13.9%), as shown in Figure 1A. Moreover, the western blot (WB) assay results indicated significant inhibition of the expression of SIRT7 and its candidate downstream target genes (γH2AX, PARP1 and XRCC6) in the 10^{10}, 5×10^{10} and 10^{11} particles/ml groups compared with the 0 particles/ml group (Figure 1B-C). The expression of

antiapoptotic markers (SURVIVIN and BCL2) was significantly increased in the 10^{11} particles/ml group compared with the 0 particles/ml group (Figure 1D-E). The expression of apoptotic markers (FAS and CASPASE8) was significantly decreased in the 10^{10}, 5×10^{10} and 10^{11} particles/ml groups compared with the 0 particles/ml group (Figure 1F-G). Taken together, the results show that hUMSC-Exos improved proliferation and suppressed apoptosis in CTX-damaged hGCs *in vitro* in a dose-dependent manner. Moreover, hUMSC-Exos suppressed the expression of SIRT7 and its candidate downstream target genes in CTX-treated hGCs *in vitro*. Among the four doses, 10^{11} particles/ml hUMSC-Exos showed the most effective rescue outcomes.

To further investigate the optimal dose of hUMSC-Exos for the treatment of POI disease, four doses of hUMSC-Exos were injected into the ovaries of CTX-treated POI model mice (POI mice). The injected exosomes were observed and traced in the ovaries of POI mice by labeling them with CM-Dil dye, as shown in Figure 2A. At 28 days after hUMSC-Exos treatment, the POI mice were sacrificed, and their ovaries were sectioned and stained for the ovarian marker MVH and the proliferation marker BrdU. Immunofluorescence images showed that $BrdU^+$ cells were rarely observed in the POI ovaries of the 0 and 10^{11} particles/ml treatment groups. The percentage of $BrdU^+$ cells in POI ovaries was dramatically increased in the 10^{12} particles/ml group compared with the 0, 10^{11} and 5×10^{11} particles/ml groups (Figure 2B). In addition, the protein levels of SIRT7 and its candidate downstream target genes (γH2AX, PARP1, and XRCC6) in ovaries were significantly repressed in the 5×10^{11} and 10^{12} particles/ml groups compared with the 0 particles/ml group (Figure 2C-D). Furthermore, the expression of antiapoptotic markers (NANOS3 and BCL2) in CTX-damaged ovaries was significantly increased after treatment with hUMSC-Exos at the 10^{11}, 5×10^{11} and 10^{12} particles/ml concentrations (Figure 2E-F). The expression of apoptotic markers (FAS and CASPASE8) in CTX-damaged ovaries was significantly decreased after treatment with 5×10^{11} and 10^{12} particles/ml hUMSC-Exos (Figure 2G-H). In summary, hUMSC-Exos injection upregulated proliferation rates and downregulated apoptosis rates in POI mouse ovaries in a dose-dependent manner. Additionally, hUMSC-Exos ovarian injection inhibited the expression of SIRT7 and its candidate downstream target genes in POI mouse ovaries. Among the four doses, 10^{12} particles/ml hUMSC-Exos injection showed the most beneficial restorative effect.

3.2 | miRNA Expression Profile of hUMSC-Derived Exosomes

The small RNA expression profile of hUMSC-Exos was investigated using Illumina HiSeq 2500 high-throughput sequencing (miRNA-seq). A total of six exosome samples were harvested from hUMSCs and human dermal fibroblasts (HDFs). Hierarchical clustering analysis showed different miRNA expression signatures between hUMSC-Exos and HDF-Exos samples (Figure 3A). The 6 most abundant miRNAs in the hUMSC-Exos samples included miR-199a-5p, miR-100-5p, miR-224-5p, miR-17-5P, miR-370-3p and miR-409-3p (Figure 3A). Real-time qPCR analysis was conducted to further determine the levels of these 6 highly expressed miRNAs. miR-17-5P exhibited the highest fold elevation (approximately 10-fold) among these top 6 miRNAs enriched in hUMSC-Exos samples (Figure 3B). Kyoto Encyclopedia of Genes and Genomes (KEGG) analysis highlighted the top 20 pathways that were strongly activated in hUMSC-Exos samples, which were associated with cell proliferation (PI3K-AKT signaling pathway, cell growth and death) and OS (Notch signaling pathway, aging), as shown in Figure 3C. According to computational prediction analysis, miR-17-5P inhibits SIRT7 expression by binding to the 3′ untranslated region (3' UTR) of SIRT7 mRNA. Additionally, the target site of miR-17-5P is highly conserved among vertebrates (Figure 3D). Collectively, the miRNA-seq results indicated the critical role of exosomal miR-17-5P among hUMSC-Exos and its candidate downstream target, SIRT7.

3.3 | miR-17-5P Mediated the Ameliorative Effect of hUMSC-Exos on a CTX-Induced POI Mouse Model

Then, hUMSC-Exos or hUMSC-$Exos^{anti\text{-}miR\text{-}17\text{-}5p}$ were injected into the ovaries of POI model mice at a concentration of 10^{12} particles/ml (for the Exos/POI and $Exos^{anti\text{-}miR\text{-}17\text{-}5p}$/POI groups, respectively). A CTX-damaged POI mouse model group with no treatment (the POI group) was used as a negative control. The restorative effect of exosomal miR-17-5P on ovarian phenotype was assessed by counting follicles and measuring the hormone levels, weights and sizes of ovaries in POI mice at 14 and 28 days after injection. Our results showed that the numbers of antral and total follicles were progressively and significantly increased in the ovaries of the Exos/POI group compared with those of the normal group (NG) and the $Exos^{anti\text{-}miR\text{-}17\text{-}5p}$/POI group from 14 to 28 days post treatment (Figure 4A-B). The sizes and weights of POI ovaries were significantly increased in the hUMSC-Exos group compared with the hUMSC-$Exos^{anti\text{-}miR\text{-}17\text{-}5}$ group at 28 days post treatment (Figure S2A).

The serum hormone levels and fetus numbers of mice were measured at 28 days after injection to illustrate the rescue effect of exosomal miR-17-5P on ovarian function. According to the hormone test results, the serum levels of E2 and AMH were significantly and progressively elevated in the hUMSC-Exos group compared with the POI and hUMSC-$Exos^{anti\text{-}miR\text{-}17\text{-}5p}$ groups from 2 to 4 weeks post injection (Figure 4C and E). In contrast, the serum level of FSH was significantly and progressively downregulated in the hUMSC-Exos group compared with the POI and hUMSC-$Exos^{anti\text{-}miR\text{-}17\text{-}5p}$ groups from 2 to 4 weeks post injection (Figure 4D). Counting of fetus numbers revealed that the hUMSC-Exos group showed better reproductive function than the POI and hUMSC-$Exos^{anti\text{-}miR\text{-}17\text{-}5p}$ groups (Figure S2B).

The proliferation and apoptosis rates of ovarian cells were also examined. The FACS results showed that the percentage of $KI67^+$ cells among ovarian cells was significantly increased and that the percentage of ANNEXIN V^+ cells among ovarian cells was significantly decreased in the hUMSC-Exos group ($KI67^+$ cells 68.29%, ANNEXIN

V^+ cells 4.53%) compared with the POI group ($KI67^+$ cells 7.21%, ANNEXIN V^+ cells 78.15%) and the hUMSC-$Exos^{anti\text{-}miR\text{-}17\text{-}5p}$ group ($KI67^+$ cells 9.96%, ANNEXIN V^+ cells 62.44%), as shown in Figure 4F-G. In summary, hUMSC-Exos preserved ovarian proliferation, phenotype and function by delivering miR-17-5P.

3.4 | hUMSC-Exos Repressed ROS Accumulation in POI hGCs and Oocytes by Delivering miR-17-5P

Since OS is involved in the pathology of POI, the ROS levels in POI models after hUMSC-Exos treatment were detected. To investigate the regulatory role of miR-17-5P, hUMSC-Exos and hUMSC-$Exos^{anti\text{-}miR\text{-}17\text{-}5p}$ were added to the culture medium of POI hGCs (for the Exos/POI and $Exos^{anti\text{-}miR\text{-}17\text{-}5p}$/POI groups, respectively). The ROS level in CTX-damaged hGCs (79%) was dramatically decreased to 8% after treatment with hUMSC-Exos. In addition, the ROS level in the Exos/POI group was significantly lower than that in the $Exos^{anti\text{-}miR\text{-}17\text{-}5p}$/POI group (70%), as shown in Figure 5A. An *in vitro* starvation-induced OS-activated POI model was established by culturing hGCs with FBS-free medium for 48 h. Then, hUMSC-Exos or hUMSC-$Exos^{anti\text{-}miR\text{-}17\text{-}5p}$ were added to the culture medium. According to our results, energy metabolism-related substances (triacylglycerol [TAG], glycogen, trehalose and glucose) in starved hGCs were significantly increased after treatment with hUMSC-Exos for 24 to 48 h. These energy metabolism-related substances were significantly elevated in the Exos/POI group compared with the $Exos^{anti\text{-}miR\text{-}17\text{-}5p}$/POI group (Figure 5B-E). The expression of ROS and SIRT7 were tested in POI mouse oocytes, Exos/POI and $Exos^{anti\text{-}miR\text{-}17\text{-}5p}$/POI group by immunofluorescence assay (Figure 5F). The resutls elucidated the significantly downregulated ROS levels and SIRT7 expression in oocytes in the Exos/POI group compared with the POI and $Exos^{anti\text{-}miR\text{-}17\text{-}5p}$/POI treatment groups (Figure 5G-H). In summary, our results demonstrated the critical role of exosomal miR-17-5P from hUMSC-Exos in repressing ROS levels in POI hGCs and oocytes.

3.5 | Exosomal miR-17-5P Inhibited SIRT7 Expression and Suppressed ROS Accumulation in a CTX-Induced POI Mouse Model

To verify that SIRT7 is the target of miR-17-5P, hUMSC-Exos and hUMSC-$Exos^{anti\text{-}miR\text{-}17\text{-}5p}$ were injected into the ovaries of POI model mice, and the expression of SIRT7 and its candidate downstream target genes (γH2AX, PARP1, and XRCC6) was detected. To set up a negative control group, CTX-induced POI model mice were given no treatment (the POI group). According to our WB results, the protein levels of SIRT7, γH2AX, PARP1 and XRCC6 in the ovaries of the Exos/POI group mice were all 2-fold lower than those in the ovaries of the $Exos^{anti\text{-}miR\text{-}17\text{-}5p}$/POI group mice (Figure 6A-D). The expression of SIRT7, γH2AX, PARP1 and XRCC6 were tested in POI mouse ovary, Exos/POI and $Exos^{anti\text{-}miR\text{-}17\text{-}5p}$/POI group by immunofluorescence assay (Figure 5E). Immunofluorescence photographs of mouse ovaries showing significantly decreased luciferase activity associated with SIRT7, γH2AX, PARP1 and XRCC6 expression in the Exos/POI group compared with the $Exos^{anti\text{-}miR\text{-}17\text{-}5p}$/POI group (Figure 6 and6G). Moreover, the FACS results indicated that ROS levels in ovaries were significantly attenuated in the Exos/POI group compared with the $Exos^{anti\text{-}miR\text{-}17\text{-}5p}$/POI group (Figure 6H). Collectively, our results indicated that SIRT7 is the target of exosomal miR-17-5P. In addition, hUMSC-Exos repressed ROS accumulation by delivering miR-17-5P.

3.6 | Exosomal miR-17-5P Downregulated PARP1, γH2AX, and XRCC6 Expression and ROS Accumulation by Inhibiting SIRT7

First, the regulatory role of miR-17-5P in suppressing the expression of SIRT7 and its candidate target genes (PARP1, γH2AX, and XRCC6) was further demonstrated in POI hGCs by the WB method. hUMSC-Exos (for the Exos group), hUMSC-$Exos^{anti\text{-}miR\text{-}17\text{-}5p}$ (for the $Exos^{anti\text{-}miR\text{-}17\text{-}5p}$ group) and hUMSC-Exos with exosomal inhibitor (for the Exos/i group) were added to culture medium of POI hGCs. POI hGCs with PBS treatment were used as negative controls (the PBS group). Normal hGCs with no CTX or exosome treatment were used as positive controls (NG). The results showed that the expression of SIRT7, PARP1, γH2AX and XRCC6 was significantly suppressed in the Exos treatment group compared with the $Exos^{anti\text{-}miR\text{-}17\text{-}5p}$ and Exos/i treatment groups (Figure 7 A-D).

Next, to unveil the SIRT7 downstream regulatory pathways, the expression of SIRT7 in normal hGCs was knocked down (producing hGCs-$SIRT7^{KD}$) and overexpressed (producing hGCs-$SIRT7^{OE}$) using siRNA and a retrovirus, respectively. The protein levels of SIRT7, PARP1, γH2AX and XRCC6 in normal hGCs were 2.5-fold, 2-fold, 2-fold and 2-fold decreased in hGCs-$SIRT7^{KD}$ (Figure 7E-H) and 2-fold, 3-fold, 2-fold and 2-fold increased in hGCs-$SIRT7^{OE}$, respectively (Figure 7I-L). In addition, the expression levels of SIRT7, PARP1, γH2AX and XRCC6 in hGCs-$SIRT7^{KD}$ were 2-fold, 4-fold, 5-fold and 3-fold lower, respectively, after Exos treatment than after $Exos^{anti\text{-}miR\text{-}17\text{-}5p}$ treatment (Figure 7E-H), while the expression levels of these molecules in hGCs-$SIRT7^{OE}$ were 3-fold, 2-fold, 3-fold and 2-fold higher, respectively, after Exos treatment than after $Exos^{anti\text{-}miR\text{-}17\text{-}5p}$ treatment (Figure 7I-L).

After exosome treatment, the ROS levels in hGCs-$SIRT7^{KD}$ and hGCs-$SIRT7^{OE}$ were also analyzed. The FACS results revealed that ROS levels were greatly increased in hGCs-$SIRT7^{KD}$ (42.25%) and hGCs-$SIRT7^{OE}$ (81.23%) compared with normal hGCs (11.56%, Figure 7M and N). In addition, the ROS levels in hGCs-$SIRT7^{OE}$ treated with hUMSC-Exos (18.66%) were dramatically lower than those in hGCs-$SIRT7^{OE}$ treated with hUMSC-$Exos^{anti\text{-}miR\text{-}17\text{-}5p}$ (80.25%, Figure 7M). The ROS levels in hGCs-$SIRT7^{KD}$ treated with hUMSC-Exos (13.22%) were dramatically lower than those in hGCs-$SIRT7^{KD}$ treated with hUMSC-$Exos^{anti\text{-}miR\text{-}17\text{-}5p}$ (43.58%, Figure 7N). Taken together, our results demonstrated that hUMSCs repressed the expression of SIRT7, PARP1, γH2AX and XRCC6 in POI hGCs by

delivering exosomal miR-17-5P. SIRT7 was the upstream regulator of PARP1, γH2AX and XRCC6. Furthermore, exosomal miR-17-5P suppressed ROS accumulation by inhibiting SIRT7.

4 | DISCUSSION

In this study, the rescue effect of exosomes from hUMSCs on POI was demonstrated *in vitro* and *in vivo*. The exosomes increased the proliferation rate and decreased the apoptosis rate in POI hGCs and ovaries in a dose-dependent manner (Figure 1 and 2). Consistent with our findings, hUMSCs and hUMSC-Exos have been reported to preserve ovarian function in POI mice (12,15,18,20). Previous studies have also reported that exosomes from human adipose MSCs and amniotic fluid stem cells can restore ovarian function after CTX-induced damage (18,20). In addition, the expression levels of SIRT7 and its candidate downstream target genes were downregulated after hUMSC-Exos treatment in this study. Previous studies have also supported our conclusion, reporting that SIRT7 depletion suppresses apoptosis in various kinds of cells (27-29). Overall, these results are the first to reveal the exosome-mediated therapeutic effect of hUMSCs.

Upon detecting miRNA expression profiles, we found that miR-17-5P was highly expressed in hUMSC-Exos, and we predicted SIRT7 to be the target of miR-17-5P (Figure 3). Based on the miRNA sequencing outcomes, we further verified the critical role of exosomal miR-17-5P in preserving ovarian function, phenotype and proliferation (Figure 4 and Figure S2). According to our results, exosomal miR-17-5P mediated increases in follicle number, ovarian size and fetus number after hUMSC-Exos injection (Figure 4 and Figure S2). In support of our outcomes, a previous study has shown that miR-17-5P is necessary for corpus luteum development (30). miR-17-5P has also been reported to promote proliferation and suppress apoptosis (31-33). Other miRNAs, including miR-125b-5p, miR-21, and miR-146a, have been found to be enriched in MSC-Exos, regulating inflammation, promoting proliferation and showing curative effects (34,35).

Starvation can activate OS in ovaries, leading to increased apoptosis, altered metabolism, impaired ovarian function and follicle loss (36,37). Upon knocking down miR-17-5P in hUMSCs, we elucidated that hUMSC-Exos repressed ROS levels in POI hGCs, oocytes and ovaries by delivering miR-17-5P (Figure 5 and 6). In addition, we showed that SIRT7 was the target gene of miR-17-5P in the context of OS regulation (Figure 5 and 6). Consistent with our results, sirtuins, including SIRT7, have been reported to be key activators of antioxidant and redox signaling (38,39).

To the best of our knowledge, this is the first study illustrating that exosomal miR-17-5P restores ovarian function, rescues CTX-damaged hGCs and alleviates OS by inhibiting the expression of SIRT7 and its downstream target genes (PARP1, γH2AX and XRCC6) (Figure 7). γH2AX, XRCC6 and PARP1 are critical mediators of DNA repair (25,40). The dephosphorylation of γH2AX promotes DNA double-strand break repair in oocytes (41,42). ROS induce DNA damage and activate γH2AX to inhibit cell growth (43). Moreover, γH2AX is involved in embryonic development (44), stem cell self-renewal (45) and aging (46). *XRCC6* protects cells from DNA damage by encoding the protein Ku70, which binds broken DNA ends and represses BAX-induced apoptosis (47-49). Poly (ADP-ribose) polymerase (PARP1) plays crucial roles in repairing DNA damage and facilitating cell cycle progression, follicular development and atresia formation (50). PARP inhibition also reduces ROS production (51). Previous studies have reported interactions among PARP1, γH2AX, XRCC6 and SIRT7 (26,40,52). Here, we clarified that hUMSC-Exos treatment produced a therapeutic effect and inhibited PARP1, γH2AX, and XRCC6 by delivering exosomal miR-17-5P and therefore suppressing its downstream target mRNA SIRT7.

Exosomes, which mediate cell–cell communication by delivering DNAs, RNAs and proteins, are ideal drug delivery vehicles. First, compared with stem cells, they are safe, with no tumorigenic tendencies. Second, MSC-derived nonimmunogenic exosomes are well tolerated *in vivo*, with longer circulating half-lives and lower immunogenicity than cells. Third, hUMSCs are convenient and cost-effective sources of exosomes for drug delivery. Therefore, hUMSC-Exos hold great promise as a therapeutic agents. However, there are still some obstacles to the application of hUMSC-Exos for POI treatment: a scalable and less expensive method for producing and purifying exosomes is urgently needed, and the homing and immunomodulatory effects of hUMSC-Exos need further investigation.

In conclusion, our findings reveal that hUMSC-Exos rescue POI and repress ROS accumulation by downregulating the expression of SIRT7 and its downstream target genes (PARP1, γH2AX and XRCC6) via delivery of exosomal miR-17-5P. This study not only clarifies the underlying mechanism of hUMSC-Exos treatment but also provides insight into the potential of exosomal miRNA-based therapy.

ACKNOWLEDGEMENTS

This work was supported by the grants from National Natural Science Foundation of China (81801515, 81801494, 81801478), Suzhou introduce expert team of clinical medicine (SZYJTD201708), Suzhou talent training program (GSWS2019005). Suzhou science and technology for people's livelihood (SYS2018081).

DISCLOSURE OF POTENTIAL CONFLICTS OF INTEREST

The authors declared no potential conflict of interest.

AUTHORS' CONTRIBUTIONS

C.D. and L.Z. performed the cellular and molecular assays in vivo and in vitro. Q.Z. participated in the statistical analysis and revised the manuscript. S.H. contributed to hGC and exosomes collection and purification. Q.Z. contributed to hGC purification culture. C.D. carried out the partial immunoassays. J.L., L.Z. and C.H. carried out the partial HE assays. C.Q. participated in the mice feeding. B.H. planned the experiments and drafted part of the manuscript. B.H. and H.L. planned the experiments and wrote the manuscript. All the authors read and approved the final manuscript.

ETHICS APPROVAL AND CONSENT TO PARTICIPATE

The use of human ovarian granular cells were in accordance with the relevant guidelines and regulations and the experimental protocols were approved by the Medical Ethics Committee of the Suzhou Hospital Affiliated to Nanjing Medical University (SZ-NJMU-003). All the patients provided written informed consent prior to participation in this study. Our investigation using experimental animals was conducted on the basis of the Nanjing Medical University Animal Center's specific guidelines and standards (20170480).

DATA AVAILABILITY STATEMENT

All the data generated or analyzed during this study are included in this published article.

ORCID

Boxian Huang https://orcid.org/0000-0001-9913-9077

REFERENCES

1. Jiao X, Ke H, Qin Y, Chen ZJ. Molecular Genetics of Premature Ovarian Insufficiency. *Trends in endocrinology and metabolism: TEM*. 2018; 29:795-807.
2. Kokcu A. Premature ovarian failure from current perspective. *Gynecological endocrinology: the official journal of the International Society of Gynecological Endocrinology*. 2010;26:555-562.
3. van Kasteren YM, Schoemaker J. Premature ovarian failure: a systematic review on therapeutic interventions to restore ovarian function and achieve pregnancy. *Hum Reprod Update*. 1999;5:483-492.
4. Torrealday S, Kodaman P, Pal L. Premature Ovarian Insufficiency - an update on recent advances in understanding and management. *F1000Research*. 2017;6:2069.
5. Kumar M, Pathak D, Kriplani A, Ammini AC, Talwar P, Dada R. Nucleotide variations in mitochondrial DNA and supra-physiological ROS levels in cytogenetically normal cases of premature ovarian insufficiency. *Arch Gynecol Obstet*. 2010;282:695-705.
6. Agacayak E, Yaman Goruk N, Kusen H, et al. Role of inflammation and oxidative stress in the etiology of primary ovarian insufficiency. *Turkish journal of obstetrics and gynecology*. 2016;13:109-115.
7. Ma M, Chen XY, Gu C, Xiao XR, Guo T, Li B. Biochemical changes of oxidative stress in premature ovarian insufficiency induced by tripterygium glycosides. *Int J Clin Exp Pathol*. 2014;7:8855-8861.
8. Bao R, Xu P, Wang Y, et al. Bone marrow derived mesenchymal stem cells transplantation rescues premature ovarian insufficiency induced by chemotherapy. *Gynecological endocrinology: the official journal of the International Society of Gynecological Endocrinology*. 2018;34: 320-326.
9. Wang Z, Wang Y, Yang T, Li J, Yang X. Study of the reparative effects of menstrual-derived stem cells on premature ovarian failure in mice. *Stem cell research & therapy*. 2017;8:11.
10. Ding C, Zou Q, Wang F, et al. Human amniotic mesenchymal stem cells improve ovarian function in natural aging through secreting hepatocyte growth factor and epidermal growth factor. *Stem cell research & therapy*. 2018;9:55.
11. Zhang H, Luo Q, Lu X, et al. Effects of hPMSCs on granulosa cell apoptosis and AMH expression and their role in the restoration of ovary function in premature ovarian failure mice. *Stem cell research & therapy*. 2018;9:20.
12. Yang Y, Lei L, Wang S, et al. Transplantation of umbilical cord-derived mesenchymal stem cells on a collagen scaffold improves ovarian function in a premature ovarian failure model of mice. *In Vitro Cell Dev Biol Anim*. 2019;55:302-311.
13. Lu X, Cui J, Cui L, et al. The effects of human umbilical cord-derived mesenchymal stem cell transplantation on endometrial receptivity are associated with Th1/Th2 balance change and uNK cell expression of uterine in autoimmune premature ovarian failure mice. *Stem cell research & therapy*. 2019;10:214.
14. Huang B, Lu J, Ding C, Zou Q, Wang W, Li H. Exosomes derived from human adipose mesenchymal stem cells improve ovary function of premature ovarian insufficiency by targeting SMAD. *Stem cell research & therapy*. 2018;9:216.
15. Yang Z, Du X, Wang C, et al. Therapeutic effects of human umbilical cord mesenchymal stem cell-derived microvesicles on premature ovarian insufficiency in mice. *Stem cell research & therapy*. 2019; 10:250.
16. Abreu SC, Weiss DJ, Rocco PR. Extracellular vesicles derived from mesenchymal stromal cells: a therapeutic option in respiratory diseases? *Stem cell research & therapy*. 2016;7:53.
17. Yaghoubi Y, Movassaghpour A, Zamani M, Talebi M, Mehdizadeh A, Yousefi M. Human umbilical cord mesenchymal stem cells derived-exosomes in diseases treatment. *Life Sci*. 2019;233:116733.
18. Sun L, Li D, Song K, et al. Exosomes derived from human umbilical cord mesenchymal stem cells protect against cisplatin-induced ovarian granulosa cell stress and apoptosis in vitro. *Sci Rep*. 2017;7:2552.
19. Monguio-Tortajada M, Roura S, Galvez-Monton C, et al. Nanosized UCMSC-derived extracellular vesicles but not conditioned medium exclusively inhibit the inflammatory response of stimulated T cells: implications for nanomedicine. *Theranostics*. 2017;7:270-284.
20. Xiao GY, Cheng CC, Chiang YS, Cheng WT, Liu IH, Wu SC. Exosomal miR-10a derived from amniotic fluid stem cells preserves ovarian follicles after chemotherapy. *Sci Rep*. 2016;6:23120.
21. Zhu Z, Zhang Y, Zhang Y, et al. Exosomes derived from human umbilical cord mesenchymal stem cells accelerate growth of VK2 vaginal epithelial cells through MicroRNAs in vitro. *Human reproduction (Oxford, England)*. 2019;34:248-260.
22. Bu H, Wedel S, Cavinato M, Jansen-Durr P. MicroRNA Regulation of Oxidative Stress-Induced Cellular Senescence. *Oxid Med Cell Longev*. 2017;2017:2398696.
23. Cloonan N, Brown MK, Steptoe AL, et al. The miR-17-5p microRNA is a key regulator of the G1/S phase cell cycle transition. *Genome Biol*. 2008;9:R127.
24. Fang Y, Xu C, Fu Y. MicroRNA-17-5p induces drug resistance and invasion of ovarian carcinoma cells by targeting PTEN signaling. *Journal of biological research (Thessalonike, Greece)*. 2015;22:12.
25. Vazquez BN, Thackray JK, Serrano L. Sirtuins and DNA damage repair: SIRT7 comes to play. *Nucleus (Austin, Tex)*. 2017;8:107-115.
26. Vazquez BN, Thackray JK, Simonet NG, et al. SIRT7 promotes genome integrity and modulates non-homologous end joining DNA repair. *EMBO J*. 2016;35:1488-1503.
27. Zhan L, Lei S, Li W, et al. Suppression of microRNA-142-5p attenuates hypoxia-induced apoptosis through targeting SIRT7. *Biomedicine & pharmacotherapy = Biomedecine & pharmacotherapie*. 2017;94: 394-401.
28. Wang X, Lin B, Nie L, Li P. microRNA-20b contributes to high glucose-induced podocyte apoptosis by targeting SIRT7. *Molecular medicine reports*. 16:5667-2017, 74.
29. Wang HL, Lu RQ, Xie SH, et al. SIRT7 Exhibits Oncogenic Potential in Human Ovarian Cancer Cells. *Asian Pacific journal of cancer prevention: APJCP*. 2015;16:3573-3577.
30. Donadeu FX, Schauer SN, Sontakke SD. Involvement of miRNAs in ovarian follicular and luteal development. *J Endocrinol*. 2012;215: 323-334.
31. Wu SY, Wu AT, Liu SH. MicroRNA-17-5p regulated apoptosis-related protein expression and radiosensitivity in oral squamous cell carcinoma caused by betel nut chewing. *Oncotarget*. 2016;7:51482-51493.

32. Hao MX, Wang X, Jiao KL. MicroRNA-17-5p mediates hypoxia-induced autophagy and inhibits apoptosis by targeting signal transducer and activator of transcription 3 in vascular smooth muscle cells. *Exp Ther Med*. 2017;13:935-941.
33. Zhang X, Song H, Qiao S, et al. MiR-17-5p and miR-20a promote chicken cell proliferation at least in part by upregulation of c-Myc via MAP3K2 targeting. *Sci Rep*. 2017;7:15852.
34. Fang S, Xu C, Zhang Y, et al. Umbilical Cord-Derived Mesenchymal Stem Cell-Derived Exosomal MicroRNAs Suppress Myofibroblast Differentiation by Inhibiting the Transforming Growth Factor-beta/SMAD2 Pathway During Wound Healing. *Stem Cells Translational Medicine*. 2016;5:1425-1439.
35. Li X, Liu L, Yang J, et al. Exosome Derived From Human Umbilical Cord Mesenchymal Stem Cell Mediates MiR-181c Attenuating Burn-induced Excessive Inflammation. *EBioMedicine*. 2016;8:72-82.
36. Wang JJ, Yu XW, Wu RY, et al. Starvation during pregnancy impairs fetal oogenesis and folliculogenesis in offspring in the mouse. *Cell Death Dis*. 2018;9:452.
37. Wang YY, Sun YC, Sun XF, et al. Starvation at birth impairs germ cell cyst breakdown and increases autophagy and apoptosis in mouse oocytes. *Cell Death Dis*. 2017;8:e2613.
38. Singh CK, Chhabra G, Ndiaye MA, Garcia-Peterson LM, Mack NJ, Ahmad N. The Role of Sirtuins in Antioxidant and Redox Signaling. *Antioxid Redox Signal*. 2018;28:643-661.
39. Gao M, Li X, He Y, Han L, Qiu D, Ling L, Liu H, Liu J, Gu L. SIRT7 functions in redox homeostasis and cytoskeletal organization during oocyte maturation. *FASEB journal: official publication of the Federation of American Societies for Experimental Biology*. 2018: fj201800078RR.
40. Lee N, Kim DK, Kim ES, et al. Comparative interactomes of SIRT6 and SIRT7: Implication of functional links to aging. *Proteomics*. 2014;14:1610-1622.
41. Chowdhury D, Keogh MC, Ishii H, Peterson CL, Buratowski S, Lieberman J. gamma-H2AX dephosphorylation by protein phosphatase 2A facilitates DNA double-strand break repair. *Mol Cell*. 2005;20:801-809.
42. Mayer A, Baran V, Sakakibara Y, et al. DNA damage response during mouse oocyte maturation. *Cell cycle (Georgetown, Tex)*. 2016;15:546-558.
43. Pal A, Alam S, Mittal S, et al. UVB irradiation-enhanced zinc oxide nanoparticles-induced DNA damage and cell death in mouse skin. *Mutation research Genetic toxicology and environmental mutagenesis*. 2016;807:15-24.
44. Liu J, Zhao Y, Ge W, et al. Oocyte exposure to ZnO nanoparticles inhibits early embryonic development through the gamma-H2AX and NF-kappaB signaling pathways. *Oncotarget*. 2017;8:42673-42692.
45. Turinetto V, Orlando L, Sanchez-Ripoll Y, et al. High basal gammaH2AX levels sustain self-renewal of mouse embryonic and induced pluripotent stem cells. *Stem cells (Dayton, Ohio)*. 2012;30:1414-1423.
46. Campisi J, d'Adda di Fagagna F. Cellular senescence: when bad things happen to good cells. *Nat Rev Mol Cell Biol*. 2007;8:729-740.
47. Bladen CL, Navarre S, Dynan WS, Kozlowski DJ. Expression of the Ku70 subunit (XRCC6) and protection from low dose ionizing radiation during zebrafish embryogenesis. *Neurosci Lett*. 2007;422:97-102.
48. Qin Q, Patil K, Sharma SC. The role of Bax-inhibiting peptide in retinal ganglion cell apoptosis after optic nerve transection. *Neurosci Lett*. 2004;372:17-21.
49. Matsuyama S, Palmer J, Bates A, et al. Bax-induced apoptosis shortens the life span of DNA repair defect Ku70-knockout mice by inducing emphysema. *Experimental biology and medicine (Maywood, NJ)*. 2016;241:1265-1271.
50. Wei Q, Ding W, Shi F. Roles of poly (ADP-ribose) polymerase (PARP1) cleavage in the ovaries of fetal, neonatal, and adult pigs. *Reproduction (Cambridge, England)*. 2013;146:593-602.
51. Hocsak E, Szabo V, Kalman N, et al. PARP inhibition protects mitochondria and reduces ROS production via PARP-1-ATF4-MKP-1-MAPK retrograde pathway. *Free Radic Biol Med*. 2017;108:770-784.
52. Li L, Shi L, Yang S, et al. SIRT7 is a histone desuccinylase that functionally links to chromatin compaction and genome stability. *Nat Commun*. 2016;7:12235.

SUPPORTING INFORMATION

Additional supporting information may be found online in the Supporting Information section at the end of this article.

How to cite this article: Ding C, Zhu L, Shen H, et al. Exosomal miRNA-17-5p derived from human umbilical cord mesenchymal stem cells improves ovarian function in premature ovarian insufficiency by regulating SIRT7. *Stem Cells*. 2020;9999:n/a. https://doi.org/10.1002/stem.3204

Figure 1 hUMSC-Exos inhibited apoptosis and SIRT7 expression in CTX-damaged hGCs

(A) FACS scatter plots showing that hUMSC-Exos increased the percentages of $PCNA^{+}/KI67^{+}$ cells among CTX-damaged hGCs in a dose-dependent manner.

(B) Protein-level analysis indicating that hUMSC-Exos suppressed SIRT7 expression in CTX-damaged hGCs in a dose-dependent manner.

(C) WB results illustrating that hUMSC-Exos inhibited the expression of γH2AX, PARP1 and XRCC6 in CTX-damaged hGCs in a dose-dependent manner.

(D-E) WB analysis showing that the protein levels of antiapoptotic genes (SURVIVIN and BCL2) in CTX-damaged hGCs were significantly elevated in the 10^{11} particles/ml group compared with the 0 particles/ml group.

(F-G) WB results showing that the expression of apoptotic genes (FAS and CASPASE8) was significantly elevated in CTX-damaged hGCs after treatment with 10^{11} particles/ml hUMSC-Exos. *** $P < 0.001$ vs the 0 particles/ml group. All experiments were repeated three times; the error bars indicate the SDs.

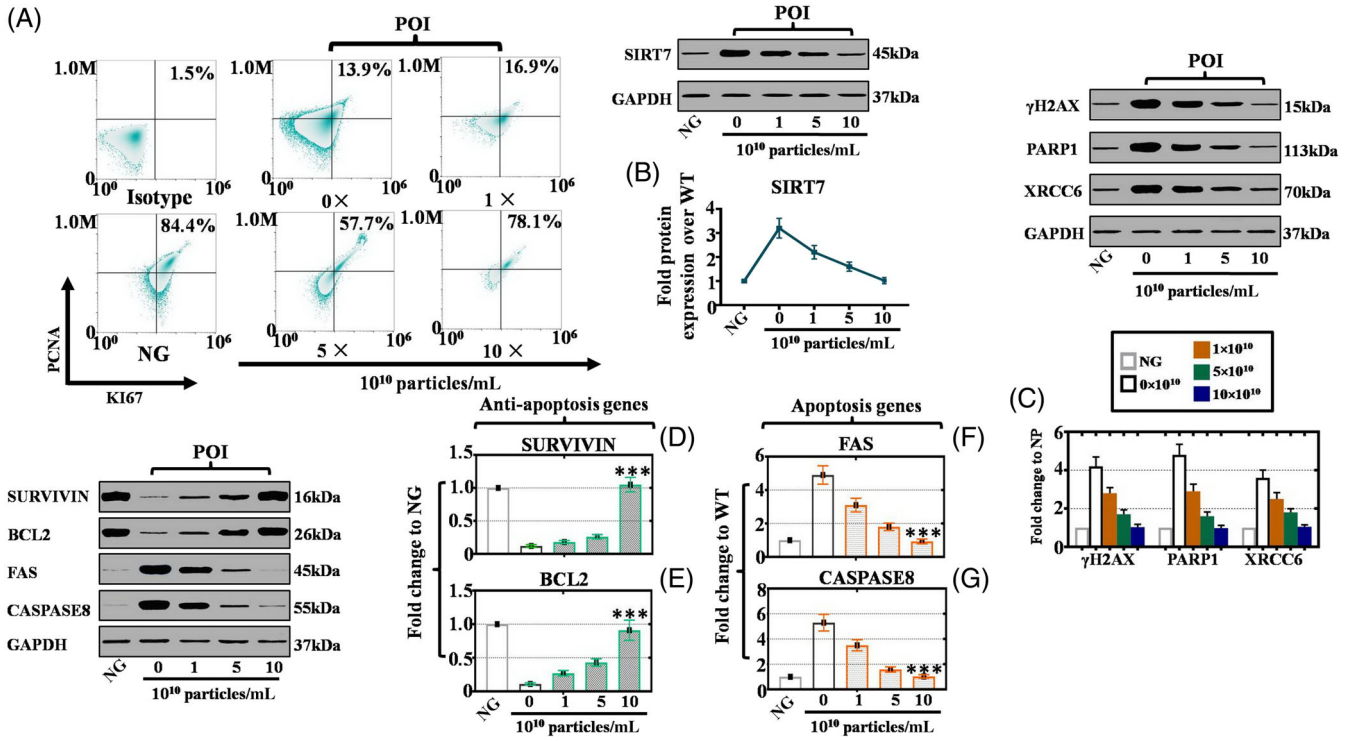

Figure 2 hUMSC-Exos repressed apoptosis and SIRT7 in the CTX-induced POI mouse model

(A) Fluorescence microscopy image of a mouse ovarian section showing the presence of the transplanted CM-Dil-labeled (red) hUMSC-Exos and the expression of BrdU (green). Scale bar = 20 μm.

(B) Fluorescence microscopy view of mouse ovarian sections showing proliferated mouse ovarian cells, as revealed by staining for MVH (red) and with BrdU (green). Scale bar = 20 μm.

(C-D) WB results illustrating that hUMSC-Exos transplantation suppressed SIRT7, PARP1, γH2AX and XRCC6 expression in the CTX-induced POI mouse model in a dose-dependent manner.

(E-F) Protein-level analysis indicating that hUMSC-Exos transplantation increased antiapoptotic gene (NANOS3 and BCL2) expression in the CTX-induced POI mouse model in a dose-dependent manner.

(G-H) Protein-level analysis indicating that hUMSC-Exos transplantation decreased apoptotic gene (BAX and CASPASE8) expression in the CTX-induced POI mouse model in a dose-dependent manner. *** $P < 0.001$ vs the 0 particles/ml group. All experiments were repeated three times; the error bars indicate the SDs.

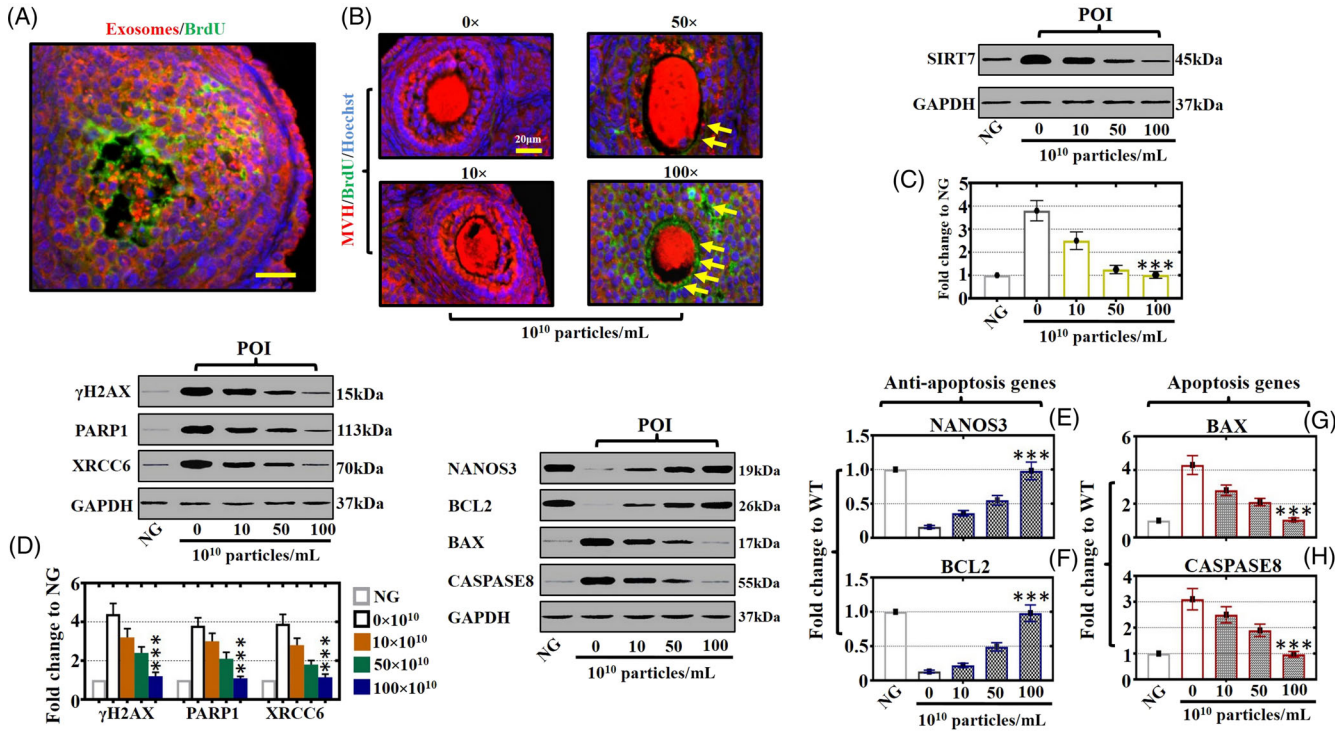

Figure 3 miRNA profile of hUMSC-Exos

(A) Heat map showing the miRNA expression profiles in three hUMSC-Exos samples and three HDF-Exos samples. The top 6 miRNAs enriched in hUMSC-Exos samples are highlighted in the box.

(B) qPCR was used to detect miRNA expression in hUMSC-Exos and HDF-Exos samples. Our outcomes demonstrated that the expression of miRNA-17-5P was 6-fold higher in hUMSC-Exos samples than in HDF-Exos samples.

(C) KEGG analysis demonstrating the top 20 pathways enriched for the miRNAs that were upregulated in hUMSC-Exos samples.

(D) Sequence alignment of miRNA-17-5P and its predicted target sites in the SIRT7 mRNA 3' UTR.

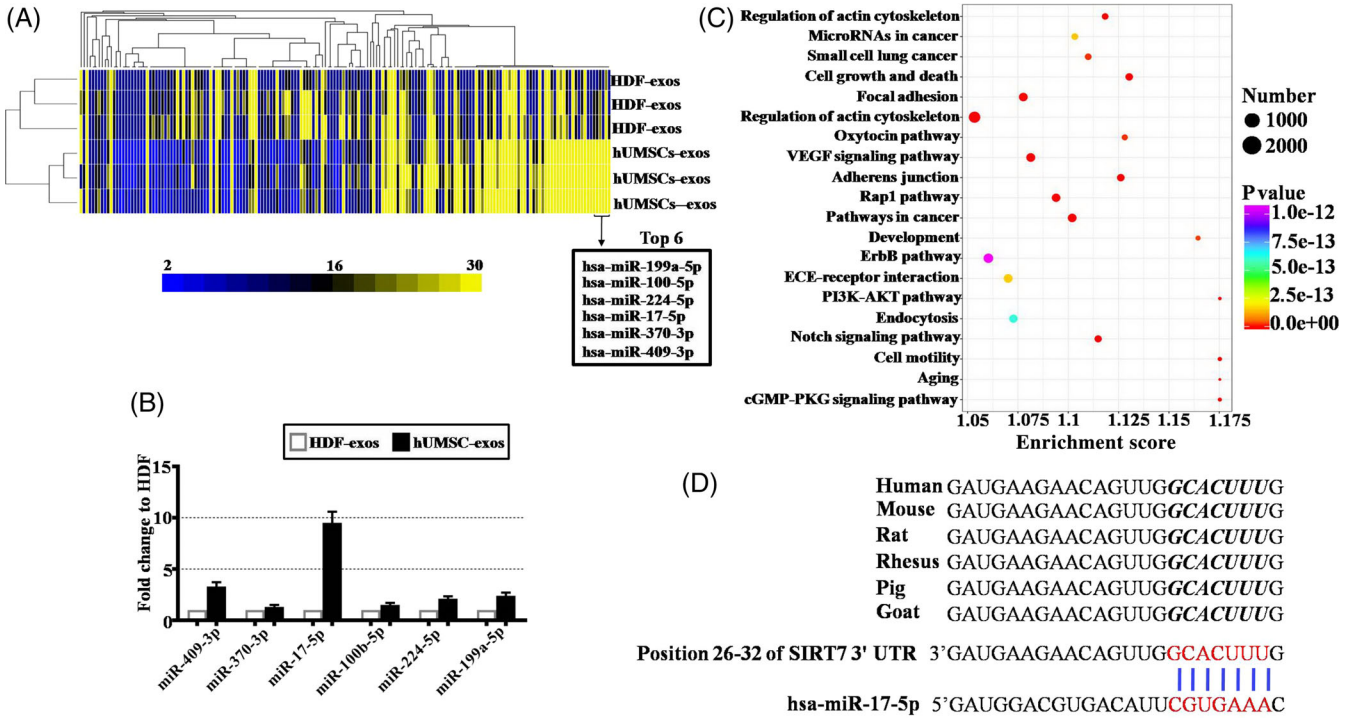

Figure 4 hUMSC-Exos restored follicular numbers and hormone levels in the CTX-induced POI mouse model by releasing miR-17-5P
(A-B) HE staining showing the morphology of follicles in different groups at 14 and 28 days after injection. Scale bars = 100 μm. The numbers of antral follicles and total follicles per ovary were determined at 28 days after injection. Our results showed that the numbers of antral and total follicles were significantly elevated in the Exos/POI group compared with the Exos$^{anti\text{-}miR\text{-}17\text{-}5p}$/POI group.
(C-E) Hormone levels in mice in different groups after transplantation. Our results showed that the serum E2 levels were significantly elevated in the Exos/POI group compared with the POI group and the Exos$^{anti\text{-}miR\text{-}17\text{-}5p}$/POI group from 1 to 4 weeks post transplantation (C). The serum FSH level was significantly repressed in the Exos/POI group compared with the POI group and the Exos$^{anti\text{-}miR\text{-}17\text{-}5p}$/POI group from 2 to 4 weeks post transplantation (D). The serum AMH level was significantly elevated in the Exos/POI group compared with the POI group and the Exos$^{anti\text{-}miR\text{-}17\text{-}5p}$/POI group from 2 to 4 weeks post transplantation (E).
(F) FACS outcomes indicating that ovarian KI67 expression was dramatically elevated in the Exos/POI group compared with the POI group and the Exos$^{anti\text{-}miR\text{-}17\text{-}5p}$/POI group.
(G) FACS outcomes illustrating that ovarian ANNEXIN V expression was dramatically downregulated in the Exos/POI group compared with the POI group and the Exos$^{anti\text{-}miR\text{-}17\text{-}5p}$/POI group. WT = wild-type mice, POI = CTX-induced POI model mice, Exos/POI = CTX-induced POI model mice treated with exosomes from hUMSCs, Exos$^{anti\text{-}miR\text{-}17\text{-}5p}$/POI = CTX-induced POI model mice treated with exosomes from hUMSCs with miR-17-5P knockdown. *** $P < 0.001$ vs the Exos/POI group. All experiments were repeated three times; the error bars indicate the SD.

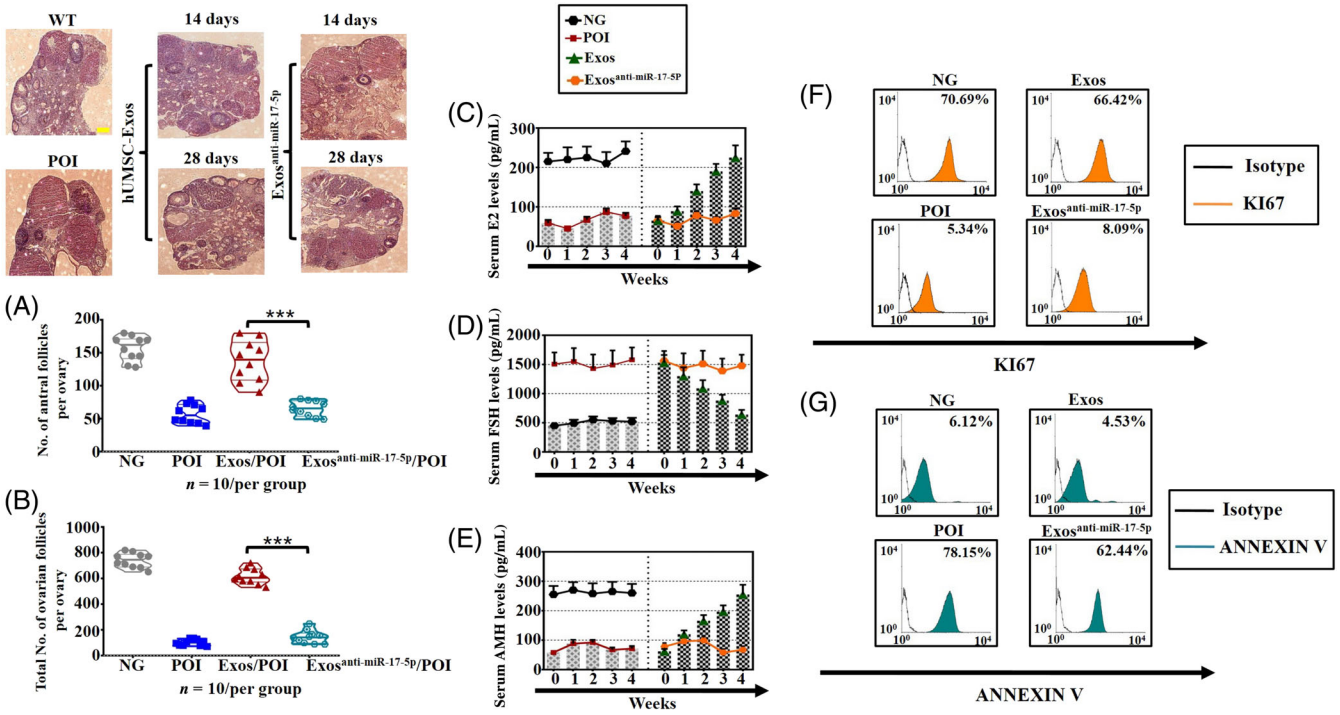

Figure 5 Exosomal miRNA-17-5P repressed ROS accumulation in CTX-treated hGCs and POI oocytes

(A) FACS outcomes showing ROS levels in CTX-damaged hGCs treated with PBS (the POI group), hUMSC-Exos (the Exos/POI group) or hUMSC-Exos$^{anti\text{-}miR\text{-}17\text{-}5p}$ (the Exos$^{anti\text{-}miR\text{-}17\text{-}5p}$/POI group).

(B-E) Metabolite assay results indicating the levels of TAG, glycogen, trehalose and glucose in starved hGCs treated with PBS (the POI group), hUMSC-Exos (the Exos/POI group) or hUMSC-Exos$^{anti\text{-}miR\text{-}17\text{-}5p}$ (the Exos$^{anti\text{-}miR\text{-}17\text{-}5p}$/POI group) from 24 to 48 h post treatment.

(F) Immunofluorescence experiment exhibited the change of expression (ROS and SIRT7) in mouse oocytes in POI, hUMSC-Exos-treated POI and hUMSC-Exos$^{anti\text{-}miR\text{-}17\text{-}5p}$-treated POI groups. Scale bars = 20 μm.

(G-H) Quantitative analysis of fluorescence intensity showing significantly downregulated ROS levels and SIRT7 expression in hUMSC-Exos-treated POI mouse oocytes compared with POI mouse oocytes and hUMSC-Exos$^{anti\text{-}miR\text{-}17\text{-}5p}$-treated POI mouse oocytes. Scale bar = 10 μm. *** $P < 0.001$. *** $P < 0.001$ vs the Exos/POI group. All experiments were repeated three times; the error bars indicate the SD.

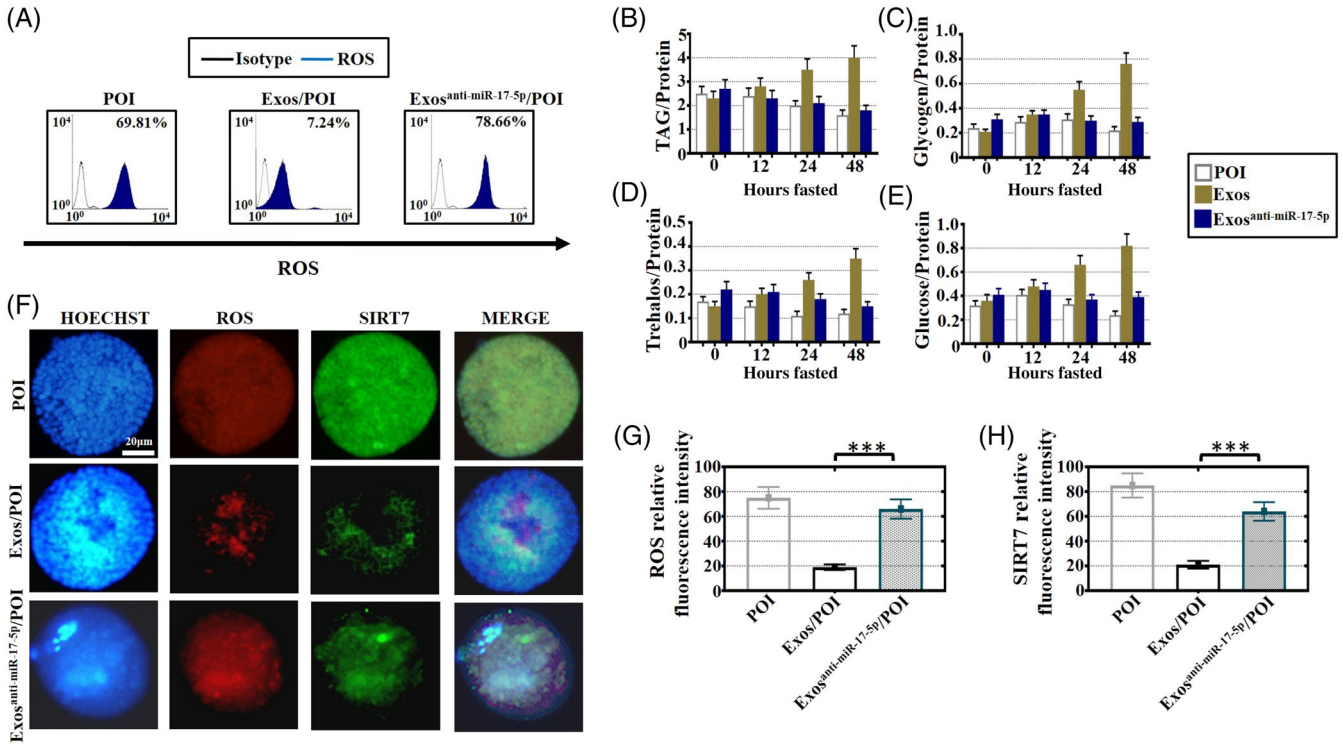

Figure 6 Exosomal miRNA-17-5P repressed ROS accumulation by regulating SIRT7 in a CTX-induced POI mouse model

(A-D) WB results indicating that ovarian SIRT7, PARP1, γH2AX and XRCC6 expression was significantly downregulated in the Exos/POI group compared with the POI and Exos$^{anti\text{-}miR\text{-}17\text{-}5p}$/POI groups.

(E) immunofluorescence experiment exhibited the change of expression (SIRT7, γH2AX, PARP1 and XRCC6) in mouse oocytes in POI, hUMSC-Exos-treated POI and hUMSC-Exos$^{anti\text{-}miR\text{-}17\text{-}5p}$-treated POI groups. Scale bar = 20 μm.

(F) Fluorescence microscopy images and quantitative analysis of fluorescence intensity showed decreased ovarian expression of SIRT7 (red) and γH2AX (green) in the Exos/POI group compared with the POI and Exos$^{anti\text{-}miR\text{-}17\text{-}5p}$/POI groups.

(G) Fluorescence microscopy images and quantitative analysis of fluorescence intensity showed decreased ovarian expression of PARP1 (red) and XRCC6 (green) in the Exos/POI group compared with the POI and Exos$^{anti\text{-}miR\text{-}17\text{-}5p}$/POI groups. Scale bar = 20 μm.

(H) FACS outcomes showing ovarian ROS levels in the POI, Exos/POI and Exos$^{anti\text{-}miR\text{-}17\text{-}5p}$/POI groups. WT = wild-type mice, POI = CTX-induced POI model mice, Exos/POI = CTX-induced POI model mice treated with exosomes from hUMSCs, Exos$^{anti\text{-}miR\text{-}17\text{-}5p}$/POI = CTX-induced POI model mice treated with exosomes from hUMSCs with miR-17-5P knockdown. *** $P < 0.001$ vs the WT group; ### $P < 0.001$ vs the Exos/POI group. All experiments were repeated three times; the error bars indicate the SDs.

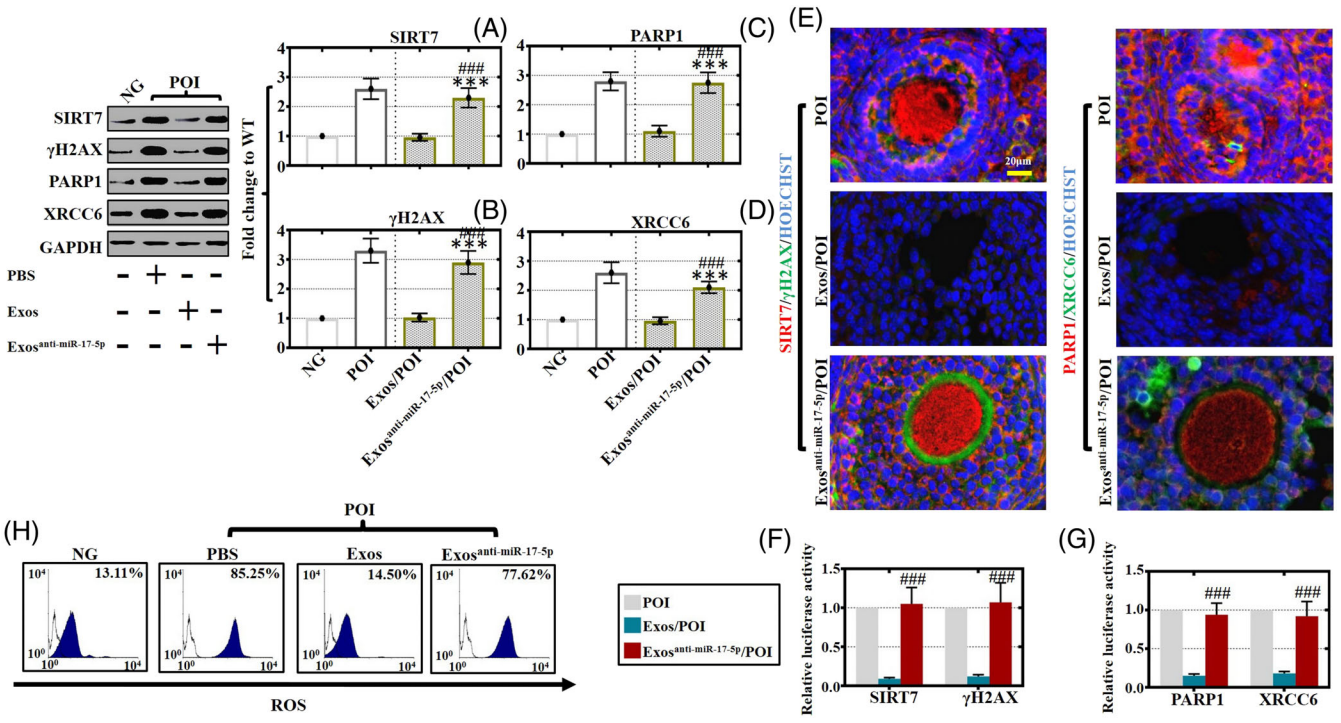

Figure 7 Exosomal miRNA-17-5P inhibited ROS and SIRT7 signaling pathways in CTX-damaged hGCs

(A) WB results indicating that SIRT7 expression was significantly downregulated in CTX-damaged hGCs treated with hUMSC-Exos compared with those treated with PBS, hUMSC-Exos+inhibitor and hUMSC-Exos$^{anti\text{-}miR\text{-}17\text{-}5p}$.

(B-D) Protein-level analysis showing that PARP1, γH2AX and XRCC6 expression was significantly downregulated in CTX-damaged hGCs treated with hUMSC-Exos compared with those treated with hUMSC-Exos+inhibitor and hUMSC-Exos$^{anti\text{-}miR\text{-}17\text{-}5p}$.

(E-H) Protein-level analysis showing that SIRT7, PARP1, γH2AX and XRCC6 expression was significantly increased in hGCs-SIRT7^{KD} treated with hUMSC-Exos$^{anti\text{-}miR\text{-}17\text{-}5p}$ compared with those treated with hUMSC-Exos.

(I-L) WB results showing that SIRT7, PARP1, γH2AX and XRCC6 expression was significantly increased in hGCs-SIRT7^{OE} treated with hUMSC-Exos$^{anti\text{-}miR\text{-}17\text{-}5p}$ compared with those treated with hUMSC-Exos.

(M-N) FACS assay results revealing the ROS levels in hGCs-SIRT7^{KD} and hGCs-SIRT7^{OE} treated with hUMSC-Exos$^{anti\text{-}miR\text{-}17\text{-}5p}$, hUMSC-Exos or PBS. *** P < 0.001 and ** *P* < 0.01 vs the Exos group. SIRT7^{KD} = SIRT7 knockdown, SIRT7^{OE} = SIRT7 overexpression, NG = normal group (containing normal hGCs with no CTX or exosome treatment), POI = CTX-damaged hGCs, PBS = hGCs treated with PBS, Exos = hGCs treated with exosomes from hUMSCs, Exos/i = hGCs treated with exosomes and exosomal inhibitor, Exos$^{anti\text{-}miR\text{-}17\text{-}5p}$ = hGCs treated with exosomes from hUMSCs with miR-17-5P knockdown. All experiments were repeated three times; the error bars indicate the SDs.

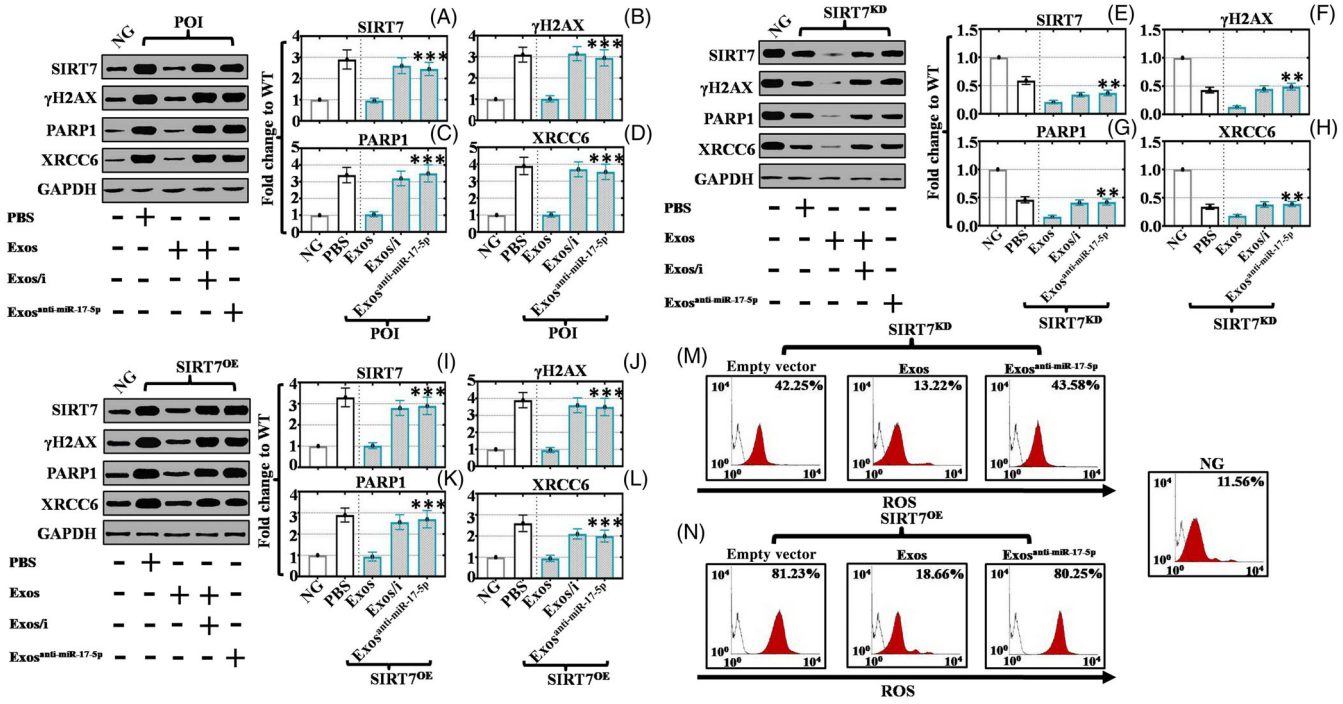

Graphical Abstract

The contents of this page will be used as part of the graphical abstract of html only.
It will not be published as part of main.

Exosomal microRNA-17-5P derived from human umbilical cord mesenchymal stem cell promotes chemotherapy-damaged human granulosa cell and ovarian cell proliferation and suppresses reactive oxygen species accumulation by repressing the expression of SIRT7 and its downstream target genes (γH2AX, PARP1 and XRCC6).